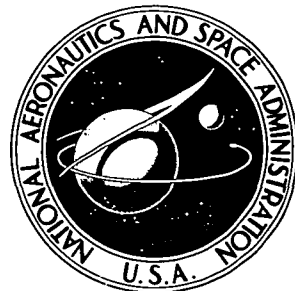


NASA TECHNICAL
MEMORANDUM

NASA TM X-3454



NASA TM X-3454

CHASE FILE
COPY

SCANNING RADIOMETER FOR MEASUREMENT
OF FORWARD-SCATTERED LIGHT
TO DETERMINE MEAN DIAMETER
OF SPRAY PARTICLES

Donald R. Buchele

*Lewis Research Center
Cleveland, Ohio 44135*



NATIONAL AERONAUTICS AND SPACE ADMINISTRATION • WASHINGTON, D. C. • NOVEMBER 1976

1. Report No. NASA TM X-3454	2. Government Accession No.	3. Recipient's Catalog No.	
4. Title and Subtitle SCANNING RADIOMETER FOR MEASUREMENT OF FORWARD-SCATTERED LIGHT TO DETERMINE MEAN DIAMETER OF SPRAY PARTICLES		5. Report Date November 1976	
		6. Performing Organization Code	
7. Author(s) Donald R. Buchele		8. Performing Organization Report No. E-8816	
		10. Work Unit No. 505-04	
9. Performing Organization Name and Address Lewis Research Center National Aeronautics and Space Administration Cleveland, Ohio 44135		11. Contract or Grant No.	
		13. Type of Report and Period Covered Technical Memorandum	
12. Sponsoring Agency Name and Address National Aeronautics and Space Administration Washington, D.C. 20546		14. Sponsoring Agency Code	
15. Supplementary Notes			
16. Abstract A scanning radiometer was built that measures forward-scattered light to determine the mean diameter of spray particles. An optical scanning method gives a continuous measurement of the light-scattering angle during spray nozzle tests. A method of calibration and a correction for background light are presented. Mean particle diameters of 10 to 500 micrometers can be measured.			
17. Key Words (Suggested by Author(s)) Particle size determination Light scattering meters Optical scanners		18. Distribution Statement Unclassified - unlimited STAR Category 35	
19. Security Classif. (of this report) Unclassified	20. Security Classif. (of this page) Unclassified	21. No. of Pages 17	22. Price* \$3.50

* For sale by the National Technical Information Service, Springfield, Virginia 22161

SCANNING RADIOMETER FOR MEASUREMENT OF FORWARD-SCATTERED LIGHT TO DETERMINE MEAN DIAMETER OF SPRAY PARTICLES

by Donald R. Buchele

Lewis Research Center

SUMMARY

One of the factors that can have a significant effect on both the performance and the pollutant emission characteristics of gas turbine combustors is the dispersion of fuel particles from the fuel nozzle. Consequently, to determine the mean diameter of spray particles, a scanning radiometer was built that measures forward-scattered light from spray particles. An optical scanning method gives a continuous measurement of the light-scattering angle during spray nozzle tests. A method of calibration and a correction for background light are presented. Mean particle diameters of 10 to 500 micrometers can be measured.

INTRODUCTION

This report describes the design of a scanning radiometer that was built for the continuous, real-time measurement of the mean diameter of liquid particles in a spray. The dispersion of fuel particles from the fuel nozzle is one of the factors that can have a significant effect on both the performance and the pollutant emission characteristics of gas turbine combustors. The effectiveness of various fuel nozzle designs has been determined in the past by direct observations and photographs of fuel or water spray patterns as well as by measurement of combustor performance.

Liquid particle diameter in the spray from a fuel nozzle can be inferred from diffractively scattered light for particle diameters greater than the wavelength of light. An optical system for the measurement of radiant flux at any small angle of forward scattering is described in references 1 and 2. Reference 1 gives a mathematical description of the scattering properties of a polydispersion of particles, and reference 2 shows the effects of different particle-diameter distributions on the light-scattering irradiance distribution. It was found that the irradiance distribution is only weakly related to the

particle-diameter distribution. The irradiance distribution can be used to determine the Sauter mean particle diameter, which is defined as the ratio of total particle volume to total particle surface area of all particles surveyed. The Sauter mean diameter was found to be less sensitive to particle-diameter distribution than were other geometric quantities of the spray particles, such as the arithmetic mean diameter and the mean diameter based on the ratio of the total surface area to the total diameter of the drops in the spray.

In developing fuel spray nozzles for gas turbine combustors, one experimental method is to test the nozzles with water in an air stream. These test results can characterize the spray by the Sauter mean diameter. Subsequent operating tests with fuel in a combustor determine the combustor performance and the pollutant emission concentrations that are related to the Sauter mean diameter. To minimize the duration of this type of test program, the scanning radiometer was designed for continuous real-time measurement.

INSTRUMENT DESIGN

Light-Scattering Equations

An optical system described in references 1 and 2 for measurement of the radiant flux at any small angle of forward scattering is shown in figure 1. Light from a point source is collimated by lens A, passes through test section B, and is focused to a point by lens C. It can be shown that light scattered anywhere in the test section at an angle θ intersects the focal plane D at a distance y from the focal point. Thus,

$$\theta = \frac{y}{f} \quad (1)$$

for $y/f \ll 1$, where f is the lens focal length. (Symbols are defined in the appendix.)

Reference 2 shows that one irradiance distribution function closely approximates actual irradiance distributions for a variety of particle-diameter distributions provided that no particles exist with a diameter larger than approximately 10 times the mean diameter of the particles. This irradiance distribution $H(P)$ for a polydiameter spray is shown in figure 2, where the abscissa that relates the measured beam-spread angle θ to the Sauter mean particle diameter D_{32} is

$$P = \frac{\pi D_{32} \theta}{\lambda} \quad (2)$$

where λ is the wavelength of the source light and $D_{32} > \lambda$. Since the distribution function $H(P)$ is known, measurement of angle θ at a preset value of H , say 0.3 to 0.5, determines P from figure 2, and D_{32} is then calculated by equation (2).

The instrument described in this report continuously measures θ by using the optical system of figure 1 and a scanning method to be described. A method of calibration and a correction for background light are presented. This instrument was designed to measure the mean particle diameter in accordance with the mean irradiance distribution curve developed in reference 2. If a diameter distribution is desired, a different optical scanner and different data-gathering electronics would be required. The design of this new equipment would depend on the analytical method used to compute the diameter distribution with acceptable accuracy from the measurements.

Description of Instrument

The optical system, with dimensions, is shown in figure 3(a). A 1-milliwatt helium-neon (He-Ne) laser with a condensing lens forms a point source of light. An aperture 0.003 centimeter in diameter intercepts stray radiation outside the point source. A collimating lens with a 7.5-centimeter-diameter aperture is smaller than the 10.0-centimeter-diameter converging lens to allow for beam spread up to 0.025 radian from scattering at the test section. A 5-centimeter-diameter lens collects all scattered light that passes through a slit on the scanning disk and focuses it on the scanning detector. This lens images the test section on the detector. Figure 3(b) shows the scanning disk with the scanning slit and a second slit with a timing detector at a larger radius to provide a timing pulse for signal conditioning. The disk rotates at 1800 rpm.

The electronic measurement circuit in figure 4(a) has signal waveforms, shown in figure 4(b), for a time spanning 1 revolution of the scanning disk. The peak of the scanner signal (1) is detected and held by the peak detector until the peak is reset to zero. The timing pulse resets the peak detector (2), thus producing the output (3) with a new peak following each scan. At the input of the comparator (4), the scanner signal (1) and a low-pass filtered fraction of peak voltage (3) as determined by the attenuator setting are compared. The fraction of voltage (3) is adjustable from 0.8 to 0.05. Whenever signal (1) is greater than signal (4), the detector output (5) is 4 volts; otherwise, it is zero. This pulse width w is the width of the scanner waveform at the preset fraction of its peak amplitude. This pulse waveform is bandpass filtered, and the amplitude of the alternating-current component at (6) is proportional to the pulse width for small ratios of pulse width w to pulse period W . The voltage at (6) is measured by a meter that can be calibrated to read D_{32} directly.

Principle of Scanning Slit

With no spray in the test section the irradiance distribution is that of the image of the source. This is illustrated in figure 5(a). This distribution can be no narrower than the Airy diffraction distribution for an ideal lens with a point source. The distribution width is further increased by the finite size of the point source of radiation, the lens aberrations, and some scattering from lens surface dirt. Spray in the test section scatters some of the light, with a distribution illustrated in figure 5(b).

When the spray is not dense, a large part of the radiation is not scattered by the spray. This light has the same irradiance distribution as existed before the spray was present, but of lower amplitude. Figure 5(c) is the sum of a reduced amplitude of 5(a), caused by scattering, plus the scattered radiation of 5(b). The measurement problem is to obtain 5(b) from measurements of 5(a) and 5(c).

The method used in the scanner is to intercept the major part of 5(a) with a stop at the axial image point of the source at plane D in figure 1. The stop size is sufficient to reduce the amplitude to 0.01 of the peak. This distribution is shown in figure 5(d). The depressed center of the curve is avoided by the design of the scanning slit (fig. 6(a)). The slit, of length A-A, is placed in an opaque rotating disk and is oriented in a radial direction. The center of the slit is covered over a length B-B to make the stop. Every point on the slit scans an off-center section of the axisymmetric irradiance distribution. These sections, such as A and B in figure 6(b), do not have a depressed center. Each of these sections has the same function, differing in relative amplitude, since the axisymmetric irradiance distribution can be accurately approximated by a Gaussian distribution and since the arc of the scanning path, because of the large radius of the scanning disk, approximates a straight line. To prove this, assume an axisymmetric Gaussian distribution of irradiance about the optical axis at C given by

$$H(x, y) = H_0 e^{-a(x^2+y^2)} = H_0 e^{-ax^2} e^{-ay^2}$$

Any off-axis section parallel to the y-axis has the same function of y multiplied by a constant that depends on x. The same result holds for a summation over any interval Δx . The Gaussian curve plotted in figure 2 closely approximates the polydiameter spray curve for amplitudes greater than 0.08 and $P \leq 2.7$. Photoelectric conversion of the flux transmitted by the scanning slit gives a curve that can be displayed on an oscilloscope for monitoring purposes.

ANALYSIS OF MEASUREMENT

Calibration

A calibration giving the mean particle diameter D_{32} in terms of the output voltage \bar{v} from the circuit in figure 4(a) is preferably done with test cells containing known-diameter latex spheres suspended in liquid. An alternative when test cells are not available is an indirect calibration. It requires an oscilloscope and a light-scattering material such as particles of silicon carbide (SiC) or aluminum oxide (Al_2O_3) grit supported between two flat windows. These particles produce light scattering similar to that from spray particles, but the scattered light does not fluctuate like that from a spray. The waveform (5) in figure 4(b) is displayed on the oscilloscope, and a ratio $(w/W)_1$ of the pulse width to the pulse period is measured. (The subscript 1 denotes calibration.) The alternating-current voltage \bar{v}_1 at (6) in figure 4(a) is also measured. This voltage \bar{v}_1 is proportional to the ratio $(w/W)_1$. Subsequent measurement of \bar{v} during a test with spray determines w/W as

$$\frac{w}{W} = \left(\frac{w}{W} \right)_1 \left(\frac{\bar{v}}{\bar{v}_1} \right) \quad (3)$$

The ratio w/W during a test is related to the distances traveled by the scanning slit as the scanner rotates. As shown in figure 4(b), waveform (4), the period W is proportional to the scanning path circumference $2\pi R$. The width w is proportional to the beam-spread width $2y$ that depends on the setting of the attenuator. Thus,

$$\frac{w}{W} = \frac{2y}{2\pi R} \quad (4)$$

Combining equations (1), (3), and (4) yields the measured beam-spread angle

$$\theta = \left[\left(\frac{\pi R}{\bar{v}_1} \right) \left(\frac{w}{W} \right)_1 \right] v \quad (5)$$

where the quantity in brackets is a calibration constant. The mean spray particle diameter D_{32} is then given in terms of the measurement voltage \bar{v} by substituting equation (5) into equation (2) to obtain

$$D_{32} = \frac{\lambda}{\pi} \left[\left(\frac{\bar{v}_1}{\pi R} \right) \left(\frac{w}{W} \right)_1 \right] \frac{P}{v} \quad (6)$$

where P is the abscissa of figure 2 corresponding to the ordinate value H selected with the attenuator at station (3) (fig. 4(a)).

Measurement Range of Mean Particle Diameter

The mean particle diameter obtained by combining equations (1) and (2) is

$$D_{32} = \frac{\lambda f}{\pi} \frac{P}{y} \quad (7)$$

The maximum measurable mean particle diameter corresponds to the smallest acceptable measurement of y , which depends on the size of the scanning slit. The minimum diameter also depends on the value of $H(P)$ and thus P in figure 2 that is selected for measurement. Because of the Gaussian approximation to the polydiameter spray curve the minimum usable value of $H(P)$ is 0.08, and thus P_{max} is 2.7. These quantities are shown in figure 7, where the scanning slit of width t and length l is displaced a distance of $\pm y$ from the optical axis. The slit displacement $\pm y$ is reached at the value of $H(P)$, and thus P , chosen for the measurement. At the limiting condition, with fixed slit dimensions and the smallest possible beam spread, the corners of the slit have the minimum irradiance level H of 0.08, where P_{max} is 2.7. The geometry of the figure gives

$$\left(\frac{P}{P_{max}} \right)^2 = \frac{y^2}{\left(\frac{l}{2} \right)^2 + \left(y + \frac{t}{2} \right)^2} \quad (8)$$

With a given P for the measurement, the maximum diameter $D_{32,max}$ is obtained by substituting equation (8) into equation (7) to eliminate y , which yields

$$D_{32,max} = \frac{2\lambda f}{\pi t} \frac{P \left[\left(\frac{P_{max}}{P} \right)^2 - 1 \right]}{1 + \left\{ \left(\frac{P_{max}}{P} \right)^2 + \left(\frac{l}{t} \right)^2 \left[\left(\frac{P_{max}}{P} \right)^2 - 1 \right] \right\}^{1/2}} \quad (9)$$

Equation (9) is plotted in figure 8 for a slit length l of 0.17 centimeter, a width t of 0.05 centimeter, a focal length f of 100 centimeters, a maximum beam-spread parameter P_{\max} of 2.7, and a wavelength λ of 0.6328 micrometer. A curve is also plotted with an l of 0.5 centimeter to show the effect of a longer slit.

The maximum θ is limited to 0.025 radian by the optical system shown in figure 3; thus, the maximum y is 2.5 centimeters by equation (1). This value substituted into equation (7) gives the minimum diameter $D_{32,\min}$ plotted in figure 8.

The results for $D_{32,\min}$ and $D_{32,\max}$ presented in figure 8 are based on strictly geometrical considerations. The particle-size measurement range can be maximized by selecting a very small value for the beam-spread parameter P since this choice will both minimize $D_{32,\min}$ and maximize $D_{32,\max}$ simultaneously. However, if P is very small, the relative irradiance that must be measured is nearly 1 (see fig. 2). To minimize the measurement error, it is desirable to use the portion of the curve of $H(P)$ as a function of P where there is appreciable slope. For the instrument just described the value selected for P was 1.2, which gives a particle-size measurement range of 10 to 475 micrometers.

Effect of Background Light

An error estimate or correction can be made for background light that was not scattered by the particles but that was scattered at optical surfaces and was not fully intercepted by the stop at the center of the scanning slit. Three additional readings are required: the peak amplitude with and without the spray and a beam-width reading without the spray.

The irradiance distribution curves of figure 2 are approximated by Gaussian curves in figure 9. The irradiance ordinate and the beam-spread abscissa are replaced with proportional voltages. Subscripts 0, t, and m represent conditions of no spray, true value with spray, and measured value with spray, respectively. The curves pass through two known points. At one point, where the abscissa v is 0, the ordinates are direct-current voltages \bar{V}_0 and \bar{V}_m measured at (7) in figure 4(a). At the second point, with an attenuation ratio k , the ordinates are direct-current voltages $k\bar{V}_0$ and $k\bar{V}_m$; the abscissas are alternating-current voltages \bar{v}_0 and \bar{v}_m simultaneously measured at (6) in figure 4(a). The true voltage to be calculated is \bar{v}_t at $k\bar{V}_t$.

For thin sprays, where the light scattered by the spray is a small fraction of the incident light, the approximation is made that the curves $V_0(v)$ and $V_t(v)$ add to produce $V_m(v)$. The true curve is thus

$$V_t(v) = V_m(v) - V_0(v) \quad (10)$$

and at $v = 0$,

$$\bar{V}_t = \bar{V}_m - \bar{V}_0 \quad (11)$$

Each curve has an equation

$$V(v) = \bar{V} e^{(v/\bar{v})^2 \ln k} \quad (12)$$

Solving equations (10) to (12) for \bar{v}_t and letting $v = \bar{v}_m$ give

$$\frac{\bar{v}_t^2}{\bar{v}_m^2} = \frac{\bar{v}_m^2 \ln k}{\ln \left[\frac{\bar{V}_m k - \bar{V}_0 e^{(\bar{v}_m/\bar{v}_0)^2 \ln k}}{\bar{V}_m - \bar{V}_0} \right]} \quad \text{for } \bar{V}_m > \bar{V}_0 \quad (13)$$

This corrected voltage can be used with equation (6) during data analysis to correct D_{32} following real-time measurements that neglect the correction.

CONCLUDING REMARKS

Tests with the radiometer using water spray have shown that it is important to protect the optical surfaces from the deposits that unconfined spray can produce. It is also desirable to minimize placing objects such as nozzles or instrumentation in the test section, where their edge diffraction can increase the amount of background light added to the measurement. Mean diameters of 75 to 150 micrometers have been recorded. Rapid changes of test conditions were possible by using real-time measurement.

Lewis Research Center,
National Aeronautics and Space Administration,
Cleveland, Ohio, July 2, 1976,
505-04.

APPENDIX - SYMBOLS

D₃₂ Sauter mean diameter of particles
f focal length of objective lens (fig. 1)
H irradiance at plane of scanning disk (fig. 3) at focal length f (fig. 1)
k voltage attenuation factor (fig. 4)
l overall slit length
P beam-spread parameter (eq. (2), fig. 2)
R rotational radius of scanning slit
t slit width
V voltage output of scanning detector
 \bar{V} peak value of V
v voltage proportional to beam-spread angle
 \bar{v} value of v with attenuation factor k times voltage \bar{V}
W pulse period of oscilloscope trace (fig. 4)
w pulse width of oscilloscope trace (fig. 4)
y ray displacement at focal length f (fig. 1)
 θ ray deviation angle at focal length f (measured beam-spread angle) (fig. 1)
 λ wavelength of source radiation

Subscripts:

m measured value with spray
t true value with spray
0 condition of no spray

REFERENCES

1. Chin, J. H.; Sliepcevich, C. M.; and Tribus, M.: Particle Size Distributions from Angular Variation of Intensity of Forward-Scattered Light at Very Small Angles. *J. Phys. Chem.*, vol. 59, Sept. 1955, pp. 841-844.
2. Dobbins, R. A.; Crocco, L.; and Glassman, I.: Measurement of Mean Particle Sizes of Sprays from Diffractively Scattered Light. *AIAA J.*, vol. 1, no. 8, Aug. 1963, pp. 1882-1886.

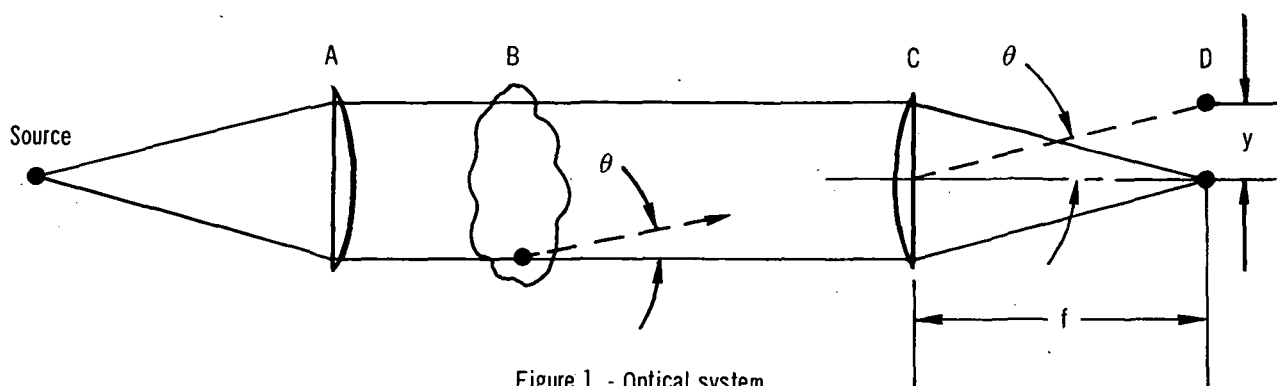


Figure 1. - Optical system.

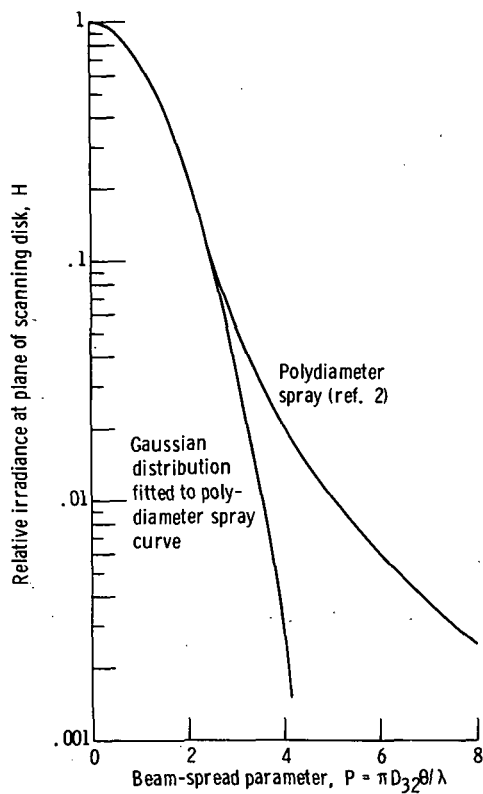


Figure 2. - Irradiance distribution for mean particle diameter D_{32} , source radiation wavelength λ , and beam-spread angle θ .

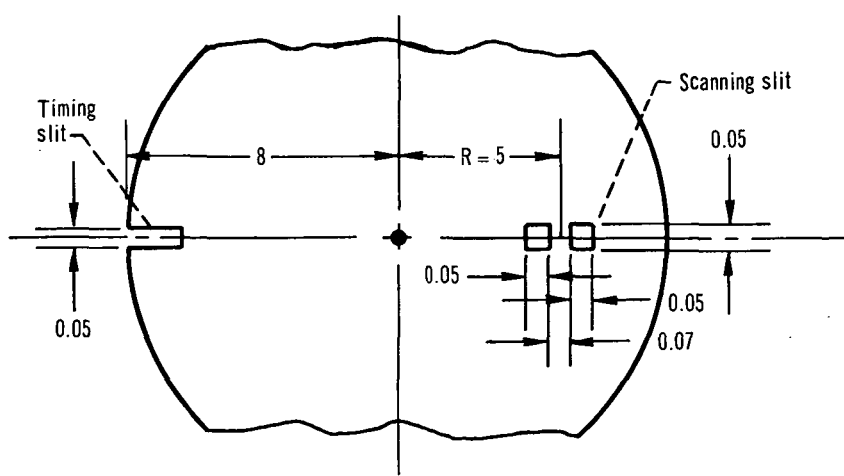
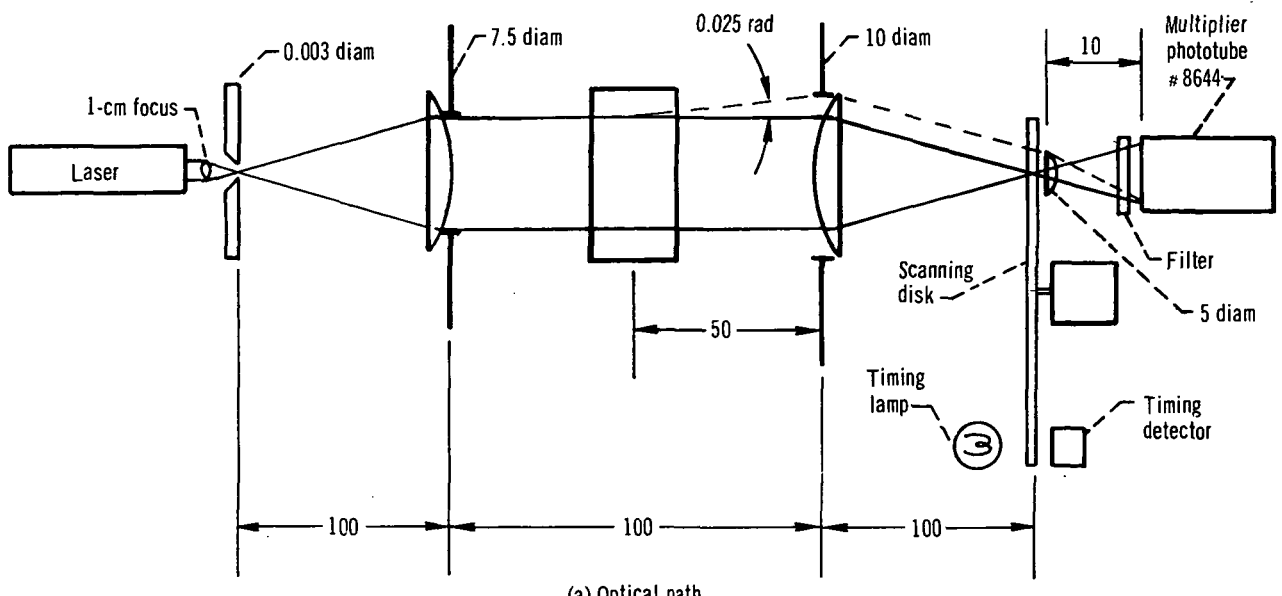
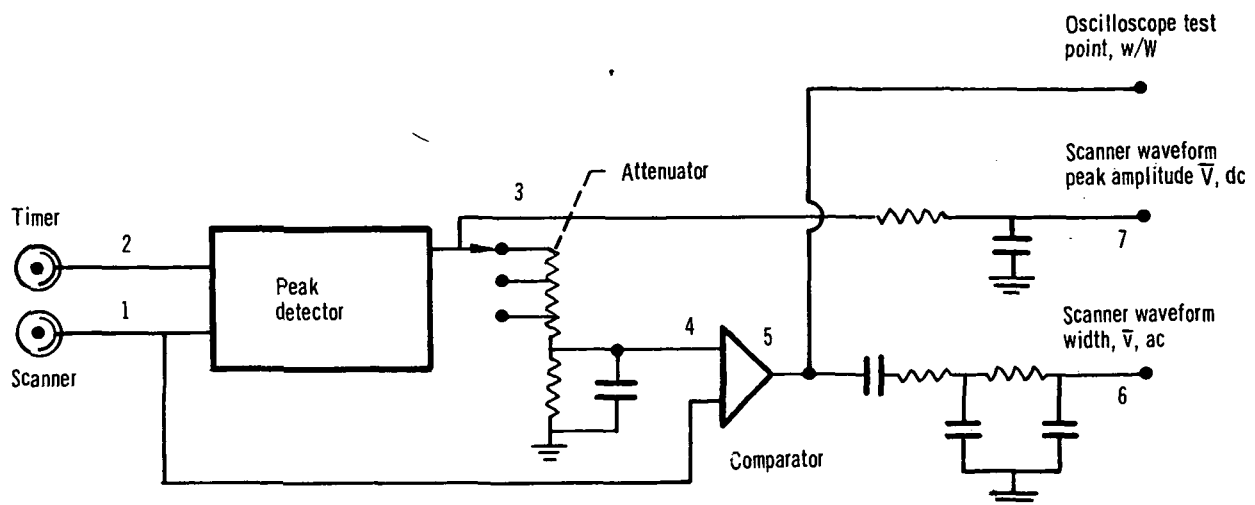
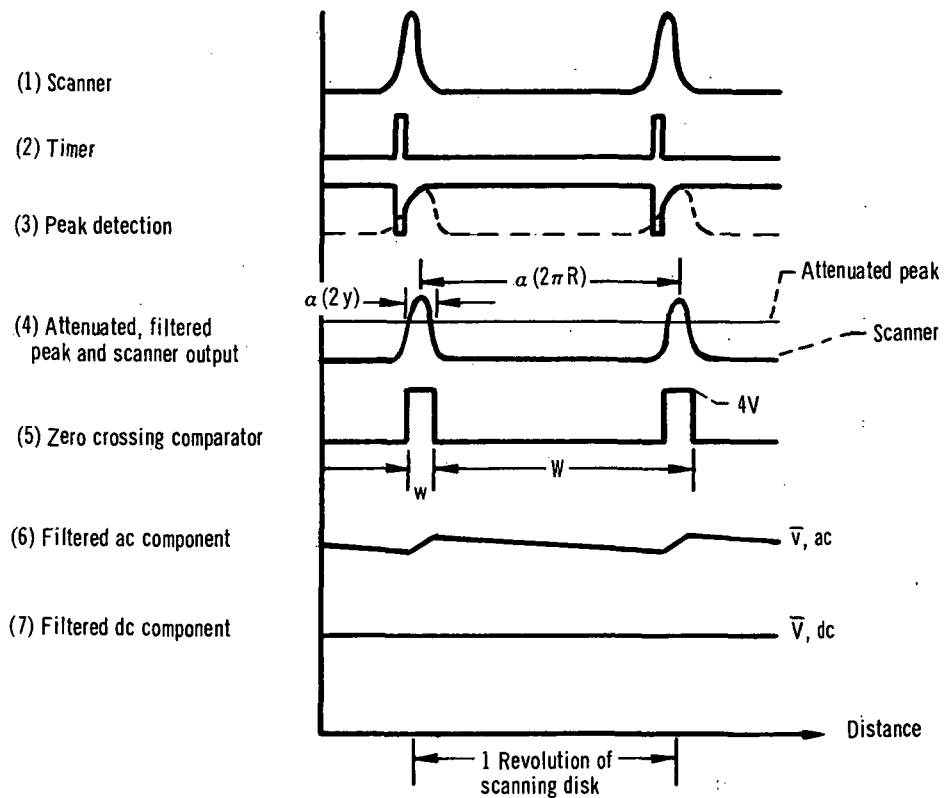


Figure 3. - Details of optical system. (Dimensions are in cm.)



(a) Electronic circuit.



(b) Signal waveforms on oscilloscope.

Figure 4. - Signal conditioning.

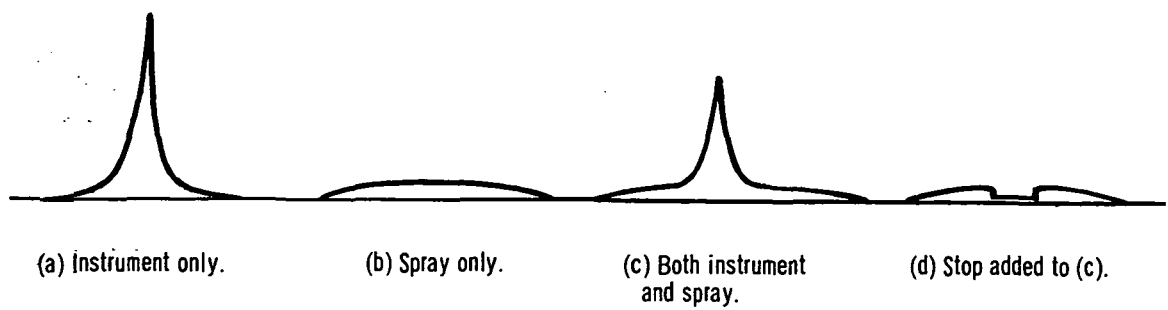


Figure 5. - Irradiance distributions.

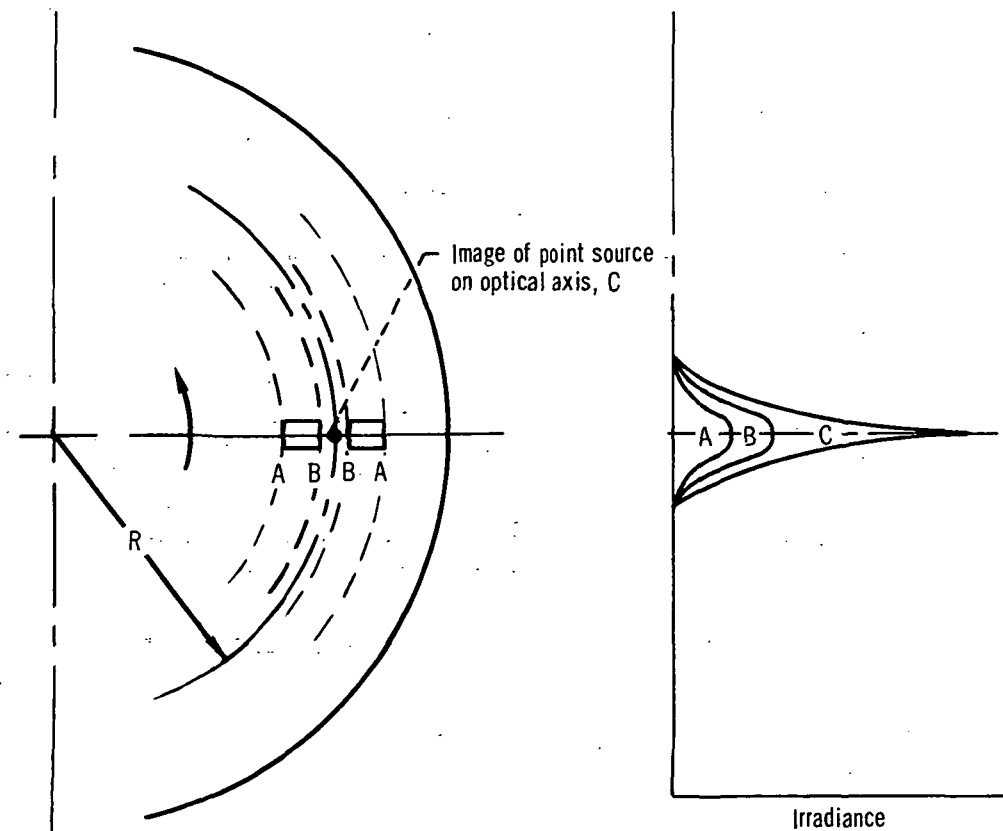


Figure 6. - Scanning disk with slit.

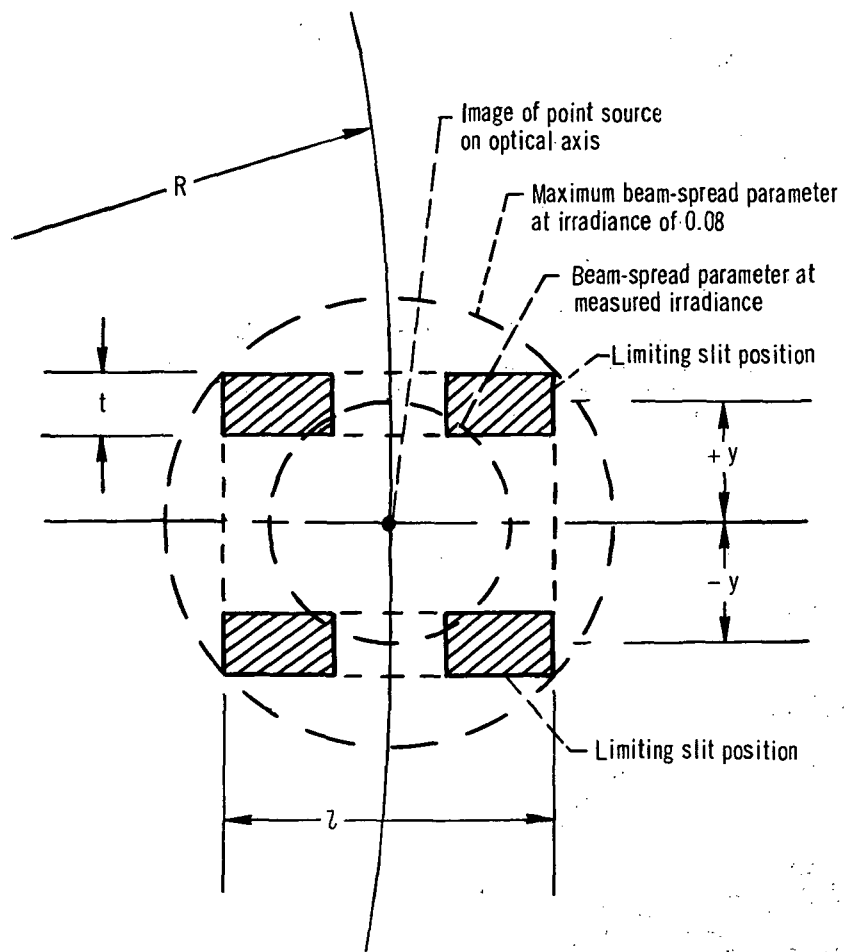


Figure 7. - Scanning slit with irradiance contours about optical axis.

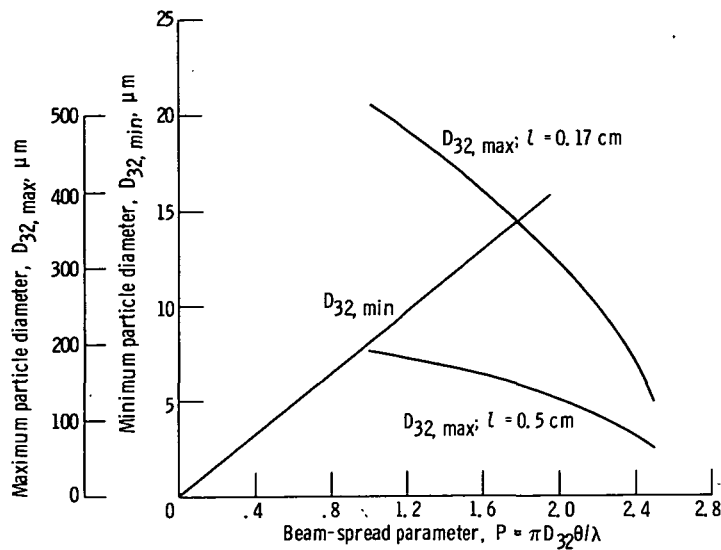


Figure 8. - Maximum and minimum mean particle diameters. Slit width, t , 0.05 cm; focal length, f , 100 cm; maximum beam-spread parameter, P_{max} 2.7; wavelength, λ , 0.6328 μm .

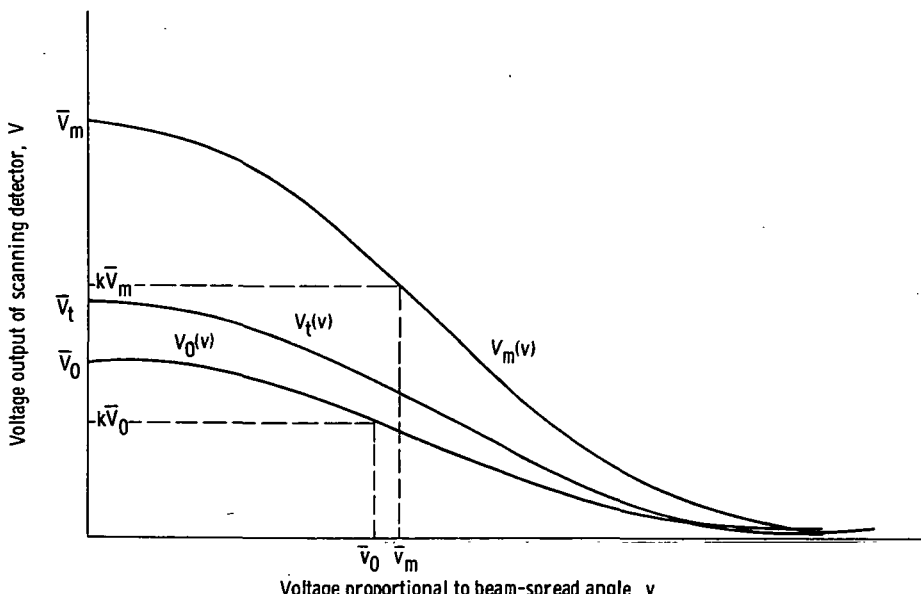


Figure 9. - Correction for background light.

NATIONAL AERONAUTICS AND SPACE ADMINISTRATION
WASHINGTON, D.C. 20546

OFFICIAL BUSINESS
PENALTY FOR PRIVATE USE \$300

SPECIAL FOURTH-CLASS RATE
BOOK

POSTAGE AND FEES PAID
NATIONAL AERONAUTICS AND
SPACE ADMINISTRATION
451



POSTMASTER : If Undeliverable (Section 158
Postal Manual) Do Not Return

"The aeronautical and space activities of the United States shall be conducted so as to contribute . . . to the expansion of human knowledge of phenomena in the atmosphere and space. The Administration shall provide for the widest practicable and appropriate dissemination of information concerning its activities and the results thereof."

—NATIONAL AERONAUTICS AND SPACE ACT OF 1958

NASA SCIENTIFIC AND TECHNICAL PUBLICATIONS

TECHNICAL REPORTS: Scientific and technical information considered important, complete, and a lasting contribution to existing knowledge.

TECHNICAL NOTES: Information less broad in scope but nevertheless of importance as a contribution to existing knowledge.

TECHNICAL MEMORANDUMS: Information receiving limited distribution because of preliminary data, security classification, or other reasons. Also includes conference proceedings with either limited or unlimited distribution.

CONTRACTOR REPORTS: Scientific and technical information generated under a NASA contract or grant and considered an important contribution to existing knowledge.

TECHNICAL TRANSLATIONS: Information published in a foreign language considered to merit NASA distribution in English.

SPECIAL PUBLICATIONS: Information derived from or of value to NASA activities. Publications include final reports of major projects, monographs, data compilations, handbooks, sourcebooks, and special bibliographies.

TECHNOLOGY UTILIZATION PUBLICATIONS: Information on technology used by NASA that may be of particular interest in commercial and other non-aerospace applications. Publications include Tech Briefs, Technology Utilization Reports and Technology Surveys.

Details on the availability of these publications may be obtained from:

SCIENTIFIC AND TECHNICAL INFORMATION OFFICE

NATIONAL AERONAUTICS AND SPACE ADMINISTRATION

Washington, D.C. 20546